

## PREPARATION SOURCE, PHYSICOCHEMICAL PROPERTIES OF CQDs AND ITS APPLICATION IN CATALYSIS AND FLUORESCENT PROBE

P. LI<sup>a</sup>, H. YANG<sup>a</sup>, B. LUO<sup>a</sup>, B. ZHOU<sup>a</sup>, S. M. AHMED<sup>a</sup>, Y. ZHANG<sup>b</sup>, S. XIA<sup>a,\*</sup>

<sup>a</sup> School of Resources and Environmental Engineering, Wuhan University of Technology, Wuhan 430070, China

<sup>b</sup>Shiyan Dongfeng equipment company, shiyan 442000, China

In recent years, carbon quantum dots (CQDs) have received due attention with the versatile application. In this paper, the carbon source of CQDs preparation was classified systematically and scientifically for the first time. The unique optical properties of CQDs were comprehensively discussed in terms of its PL intensity and UV-vis spectrum. The morphology properties of CQDs were also deduced according to their TEM profiles. The graphitization degree were characterized using Raman and XRD. In addition, the preliminary application of CQDs in the field of catalysis and fluorescent probe was illustrated. The mechanism of CQDs in these fields was developed.

(Received February 26, 2020; Accepted July 14, 2020)

*Keywords:* Carbon quantum dots, Optical properties, Morphology properties, Catalysis, Metal detection

### 1. Introduction

Carbon quantum dots (CQDs), a new type of zero-dimensional nano-carbon material, has the unique optical and other physicochemical properties [1, 2]. CQDs has been paid gradually by many researchers worldwide due to its versatile application in many fields, including biosensing, biotags, fluorescent probes and catalysis with the advantages of non-toxicity, bio-affinity and water-solubility [2-4].

In general, the material properties of CQDs depend on largely the preparation materials used for preparation of CQDs, which is called as carbon source. Therefore, the choice of carbon source plays the important role in the preparation of CQDs[5]. At present, a lots of carbon source has been developed for the preparation of CQDs[6-9]. In present, there is no detailed summary about the types of carbon sources although many different kinds of carbon sources for the preparation of CQDs. In this paper, we summarize and classify several common carbon sources.

The unique physicochemical properties are intrigued feature for CQDs, which are usually explained from the perspectives of optical properties, morphology properties and graphitization degree of CQDs[10]. For the best of our knowledge, few literature has depicted the CQDs from this four properties [11]. In this paper, we deduced several important physicochemical properties and give a reasonable explanation.

---

\* Corresponding author: xiashibin@126.com

Up to date, many studies has shown the excellent performance in catalysis, e.g., the combination of CQDs with semiconductor photocatalysts can improve the photocatalytic performance of semiconductors[12-14]. In this paper, the recent application of CQDs catalyst has been accumulated and classified according to the function of CQDs in catalysis.

The fluorescent probe method has the advantages of simple sample pretreatment, fast response, wide linear dynamic range, less spectral interference and high sensitivity, and has become a common analytical method for the rapid detection of metal ions[15, 16]. Due to the fluorescent feature of CQDs, it has been widely developed as a fluorescent probe for various quencher[17-19]. However, the mechanism of CQDs fluorescence quenching is versatile and should be concluded systematically.

Herein, the carbon sources for the preparation of CQDs were categorized and compared for four kinds according to their profile. The physicochemical properties of CQDs were illustrated explicitly. In addition, the application and mechanism of CQDs in the field of catalysis and fluorescent probe has been summarized in detail.

## **2. Preparation methods and materials for CQDs**

### **2.1. Preparation methods for CQDs**

Up to now, the methods of preparing CQDs are mainly divided into two categories: "up-bottom" and "bottom-up". The "up-bottom" method is to cut large-scale structured raw materials into small CQDs using physical or chemical methods. Typical methods include laser etching, chemical oxidation, arc discharge, and electrochemical synthesis, etc[20, 21]. The "up-bottom" method can adjust the size of the product by altering the respective reaction parameters, and controlling the boundary structure. The "bottom-up" synthesis method is to utilize small organic molecules or oligomers as the carbon source to prepare carbon through a series of chemical reactions. Common methods include microwave-assisted synthesis, hydrothermal synthesis, template, combustion, and plasma synthesis, etc[22, 23]. The preparation methods for CQDs is completely depending on the carbon source used.

### **2.2. Preparation materials for CQDs**

#### **2.2.1. Carbon-based materials**

Carbon-based materials are the primary carbon source for the preparation of CQDs in the early study stage of CQDs, which have the advantage of inexpensiveness, readily availability, non-toxicity, and no secondary process[24]. The common carbon-based materials include activated carbon, fullerene carbon, activated carbon fiber, carbon nanotube and graphene[25, 26]. In general, the "up-bottom" method was employed to prepare the CQDs using carbon-based materials, in which carbon-based materials are cut from big to small into CQDs.

Zhang et al. prepared a CQDs using fullerene charcoal as carbon source by nitric acid reflux oxidation method[27]. The resulted CQDs is capable of emitting yellow fluorescence with the quantum yield of 3%-5%. The applications in fields of life show that the CQDs prepared by fullerene charcoal have stable photoluminescence behavior in a wide pH range, high ionic strength and long-time illumination.

Yan et al. prepared a CQDs using graphene as carbon source by oxidation method [28]. The resulted CQDs was further employed to prepare a heterogeneous composite catalyst of CQDs/ZnO containing multi-layer CQDs by impregnation method. The optical and catalytic properties of the prepared catalyst were studied. The results show that CQDs/ZnO has better electron separation efficiency and lower electron-hole coupling efficiency than pure ZnO due to the interaction between CQDs and ZnO. In addition, the CQDs/ZnO heterogeneous composite catalyst exhibited stronger catalytic efficiency than ZnO in the degradation experiment of RhB.

However, the oxidant or expensive equipment is needed to prepare CQDs using carbon-based materials as carbon source. The common oxidant is nitric acid and sulfuric acid which causes great harm to the environment. Therefore, the green preparation method of CQDs, e.g., environmental-friendly oxidant and simple cut method using carbon-based materials should be developed in future.

### **2.2.2. Synthetic chemicals**

Due to the present defect of "up-bottom" method, many scholars have focused to the synthesis of CQDs by simple synthetic chemicals. Usually, "bottom-up" methods are employed to synthesize CQDs using synthetic chemicals as carbon source, in which the general method is hydrothermal synthesis. The common synthetic chemical for CQDs synthesis is citric acid[29, 30].

Bozetine et al. synthesized a CQDs by hydrothermal synthesis method using fructose as carbon source, and prepared a composite photocatalyst of CQDs/ZnO by one-step method[31]. The photocatalysis efficacy of composite material for RhB solution was studied. The results show that the degradation efficacy of RhB using CQDs/ZnO composites is better than that of ZnO. At the same time, the free radical analysis experiments show that the CQDs/ZnO composites can generate more hydroxyl radicals during catalysis period.

Shouvik et al. prepared a CQDs by hot solvent method using self-passivation PEG-200 as carbon source [32]. The biotoxicity and application in bioimaging of resulted CQDs were also studied. The results show that the obtained CQDs has a high quantum yield, fluorescence intensity and good biocompatibility, which indicates it could be employed in bioimaging of RBCs and Hep G2 cells.

Compared with carbon-based materials, the synthesis of CQDs using chemical reagents as carbon source are more simple and technic available. However, some of the organic solvents was used in CQDs synthesis to enhance the quantum yield, which at certain limit the environment-friendly utilization of CQDs.

### **2.2.3. Plant extracts**

The plant extract is a natural raw material extracted from plants. The natural plant extracts have the advantage of green, nontoxicity, easy availability and cost-efficiency. Therefore, plant extracts exhibit great promising potential in the synthesis of CQDs. The common plant extract carbon sources include leaves, fruit flesh and peel[33]. The hydrothermal synthesis method is most common employed for this carbon source.

Atchudan et al. synthesize a CQDs by hydrothermal synthesis method using peach meat as carbon source, and prepared a composite material of CQDs/TiO<sub>2</sub> by one-step method [34]. The photocatalysis efficiency for methyl blue of composite materials were studied. The degradation rate of methyl blue using CQDs/TiO<sub>2</sub> was five times higher than that of pure TiO<sub>2</sub>.

Compared to the carbon source pre-mentioned, plant extracts employed to synthesize CQDs require an additional step for plant harvesting and processing step. In addition, to obtain the plant extracts is limited largely by reason. Despite all this, this carbon source is still considered as the greenest and most admirable material for CQDs synthesis.

#### 2.2.4. Animal by-products

Similar to plant extracts, some animal by-products were also promising carbon source. The common animal by-products as carbon sources are egg, milk and honey [35-37]. The hydrothermal synthesis method is as well common used for this carbon source.

Wang et al. used milk as carbon sources to prepare CQDs by hydrothermal synthesis method, and studied the toxicity of resulted CQDs on U87 cells [38]. The results show that the CQDs are non-toxic and have very good biocompatibility, indicating CQDs prepared by milk have considerable application potential in bio-imaging.

At present, the research scope of this kind of carbon source is relatively narrow because animal by-products has a higher value and cost compared to other carbon source. This carbon source is green and valuable also, which should been paid due attention in the future.

### 3. Physicochemical properties for CQDs

#### 3.1. Optical properties for CQDs

##### 3.1.1. Excitation wavelength dependent

The most prominent feature of CQDs is excitation wavelength dependent. As shown in Fig. 1, as the increasing wavelength of the excitation spectrum, the red-shifted occurs in the emission spectrum. Excitation wavelength dependent determines the gift of tunable wavelength for CQDs[39]. However, no elusive conclusion has been made to explain the fluorescent property of CQDs. This property can be explained by the two hypotheses of quantum confinement theory and defect state emission[40, 41].

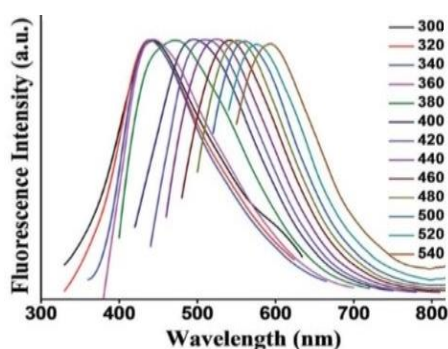


Fig. 1. Property of excitation wavelength dependent of CQDs.

It is well known that the generation of fluorescent is due to the radiative combinations of electron-hole pairs. Study has shown the surface defects on CQDs can facilitate more effective radiative combinations of surface-confined electron-holes leading to the fluorescent property of CQDs[42].

The quantum confinement theory is interpreted from in the perspective of electron transferring. The generation of fluorescent is due to the electron transferring from the lowest unoccupied molecular orbital (LUMO) to the highest occupied molecular orbital (HOMO)[43].

### 3.1.2. Up-conversion luminescence property of CQDs

Some prepared CQDs have unique up-conversion photoluminescence properties, which are capable of exciting short-wavelength visible or ultraviolet light after absorbing long-wavelength near-infrared light or visible light (as shown in Fig. 2. The up-conversion PL properties could be ascribed to the electronic anti-Stokes transition from the energy levels of  $\pi$  to  $\sigma$  due to the carbene ground-state multiplicity. Most semiconductors have a light response range of ultraviolet light or finite wavelength visible light, e.g., ZnO and Cu<sub>2</sub>O have absorption thresholds of 370 nm and 564 nm, respectively, and cannot fully utilize ultraviolet and visible light in sunlight[44, 45]. After compounding this semiconductors photocatalysts with CQDs, excited semiconductors can utilize shorter wavelengths of light radiated from the up-conversion luminescence properties of CQDs and generate more photogenerated carriers.

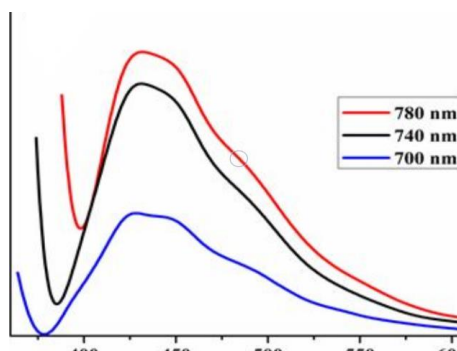


Fig. 2. Up-conversion luminescence property of CQDs.

### 3.1.3. UV-vis adsorption properties of CQDs

CQDs has the abroad UV-Vis adsorption spectrum covering the UV spectrum, visible spectrum and even near-infrared spectrum (as shown in Fig. 3 which endows the volatile application potential of CQDs in the various field, including LED light, catalysis, medical material and biomaterial[46-48]. Up to date, CQDs with the near-infrared spectrum adsorption is hot areas of research.

The CQDs showed three main character absorption peaks or should peaks at appropriate 207 nm, 251 nm and 352 nm, which are ascribed to an aromatic C=O bond ( $\pi$ - $\pi^*$  transition), C=C bonds ( $\pi$ - $\pi^*$  transition) and C=O ( $n$ - $\pi^*$  transition), respectively[49, 50].

The UV-Vis adsorption spectrum is depending on the carbon source and preparation method of CQDs. Therefore, the UV-Vis adsorption spectrum is 'tunable' as well as the excitation wavelength dependent property.

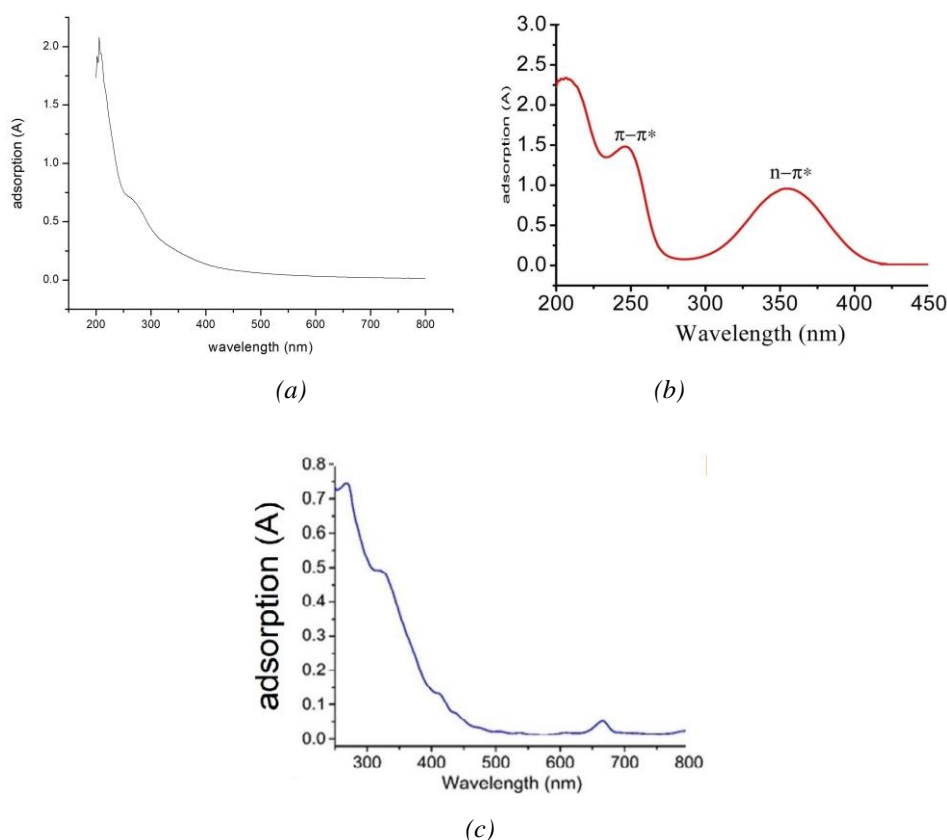


Fig. 3. UV-vis adsorption spectrum of CQDs (a UV spectrum b visible spectrum c near-infrared spectrum).

### 3.2. Morphology properties for CQDs

The particles shape/size, lattice spacing and surface defects are the important performance for CQDs. The Fig. 4 shows the TEM characteristics of walnut shell-based CQDs. Usually, CQDs belongs to the typical quasi-zero dimension material and the distributed-well CQDs exhibits the sphere-like shape with a size distribution less than 10 nm. To avoid the aggregation of CQDs, the dispersant can be used during the synthesis of CQDs. The reported CQDs has the average lattice spacing distance of 0.220 nm~ 0.320 nm, which is corresponding to the graphitic carbon or amorphous carbon[51, 52]. The surface defects are analyzed by observing the structure of lattice edge. The main surface defects of CQDs include zigzag edge and armchair edge[42, 53].

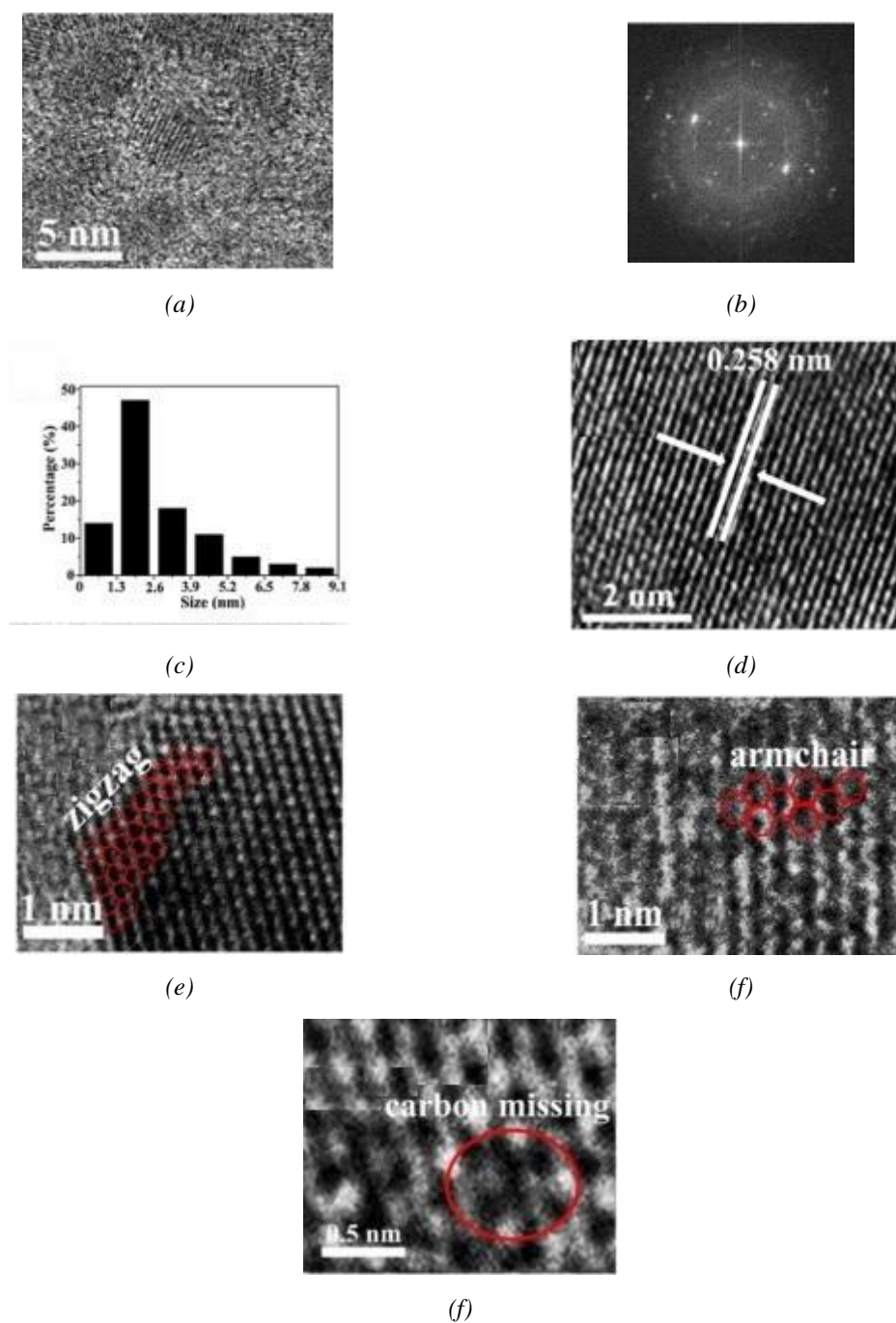


Fig. 4. The microstructural characteristics of walnut shell-based CQDs (a) HRTEM image, (b) SAED pattern, (c) particle size distribution and (d) lattice spacing of walnut shell-based CQDs. (e) Zigzag edge (f) Armchair edge and (g) defect structure in walnut shell-based CQDs.

### 3.3. Graphitization degree for CQDs

Raman is employed to analyze the graphitization degree for CQDs. The relative intensity of the D band is a reflection of the disorder of the crystal structure. The G band represents the first-order scattering E<sub>2g</sub> vibration mode, which is used to characterize the sp<sup>2</sup> bond structure of carbon. The well graphitized carbon materials have the intensities ratio of D band and G band ( $I_D/I_G$ ) to be less than 1, which indicates the less defective carbon structures of CQDs (as shown in Fig.

5 b)[54]. However, Raman is not always valid to test the graphitization degree of CQDs, as shown in Fig.6 b, which is due the strong PL properties of CQDs hindering the Raman signal[55, 56]. XRD is also used as an auxiliary to support the result of Raman. Usually, a distinct broad absorption peak appeared at approximately  $27.6^\circ$  (as shown in Fig. 5 a), indicating the amorphous carbon structure of the CQDs. In addition, the presence of diffraction peak at  $44^\circ$  corresponds to the (100) crystal plane of graphite, which means that the CQDs has a certain degree of graphitization.

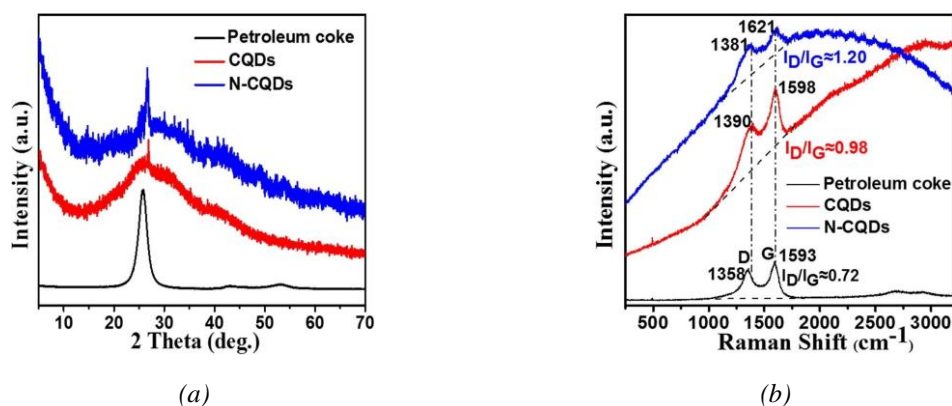


Fig. 5. XRD patterns (a) and Raman spectra (b) of petroleum coke, CQDs and N-CQDs.

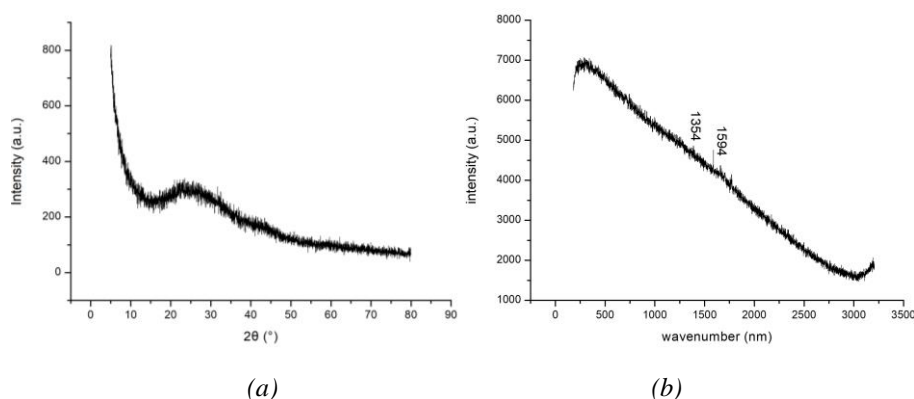


Fig. 6. XRD patterns (a) and Raman spectra (b) of LSACF based-CQDs.

## 4. Applications of CQDs in the field of catalysis

### 4.1. Traditional catalyst

Many researches show that CQDs has the ability to efficiently receive electrons, which act as a medium for electron migration during the reaction process, reducing the energy barrier between reactants and products. Therefore, CQDs could act as an effective catalyst in catalysis [57].

Edison et al. used hydrothermal synthesis to prepare CQDs using Pitaya flesh as carbon source, and studied the catalytic effect of CQDs on the reduction of methylene blue [58]. The results show that the existence of CQDs greatly accelerates the reduction process of methylene blue.

In addition, Edison et al. also prepared CQDs using kiwi meat as carbon source by hydrothermal synthesis method, and examined the catalytic effect of CQDs on the reduction process of rhodamine B [59].

#### 4.2. Photocatalyst composite

The rapid recombination of photogenerated electron-hole pairs is an important factor affecting the photocatalytic activity. Therefore, to improve the separation efficiency of photogenerated carriers in semiconductors has become a major goal of improving photocatalytic performance [60]. The surface of CQDs conjugates a large  $\pi$  bond and has good electrical conductivity. A good interfacial effect between and a semiconductor photocatalyst could be formed, which serves as an effective reservoir and conductor for photogenerated electrons, accelerating electron transfer, inhibiting photogenerated carriers, prolonging the lifetime of photogenerated carriers, and ultimately improve photon efficiency and catalytic performance [61]. The hydroxyl and carboxyl groups on the surface of CQDs can act as nucleation sites for catalytic reaction with strong interface bonding with photocatalyst [62]. In addition, due to the up-conversion effect of CQDs, the combination of CQDs could enhance the light efficiency of photocatalyst. The following describes the enhanced light performance of various CQDs/photocatalyst composite

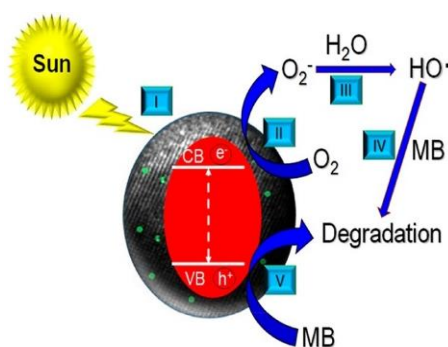


Fig. 7. Catalysis mechanism of CQDs composite photocatalyst.

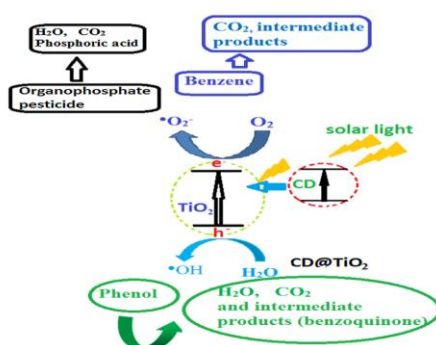


Fig. 8. Catalysis mechanism of CQDs/TiO<sub>2</sub> composite photocatalyst.

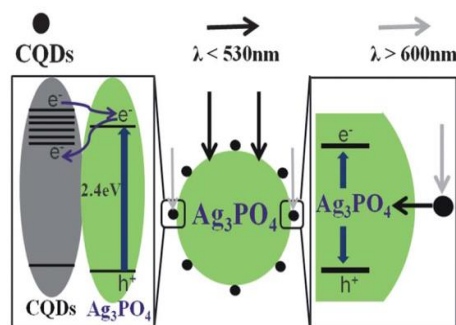


Fig. 9. Catalysis mechanism of CQDs/Ag<sub>3</sub>PO<sub>4</sub> composite photocatalyst.

Bhati et al. used the microwave radiation method to prepare CQDs using bougainvillea leaves as carbon source with the near-infrared spectrum adsorption, which was not affected by the excitation wavelength, and studied the photocatalysis ability CQDs in the sunlight [63]. The good catalytic efficiency was obtained to degrade methylene blue using CQDs as composite photocatalyst. The Fig. 7 shown the catalysis mechanism of CQDs composite photocatalyst.

Araújo et al. prepared CQDs using cotton cellulose as carbon source by hydrothermal synthesis method, and studied catalytic degradation of materials to nitrogen dyes using CQDs/Fe<sub>2</sub>O<sub>3</sub> composite photocatalyst [64]. The results show that the aggregation effect of Fe<sub>2</sub>O<sub>3</sub> is decreased and the oxygen-containing functional groups are significantly increased due to CQDs is successfully synthesized on the surface of Fe<sub>2</sub>O<sub>3</sub> which enhances the surface properties of Fe<sub>2</sub>O<sub>3</sub>. In addition, in the process of catalytic degradation of nitrogen-based dyes, the more efficient separation of photogenerated charges and lower photogenerated hole-pair recombination rate were observed.

Hazarika et al. used a hydrothermal synthesis method to prepare CQDs using citric acid as carbon sources and CQDs/TiO<sub>2</sub> composites were synthesized by in situ and ex situ [65]. The degradation effects of benzene, phenol and insecticide on the composite under solar illumination were also studied. The results show that the in-situ composite CQDs/TiO<sub>2</sub> composite exhibits the best removal effect on the above three pollutants. The Fig. 8 shown the catalysis mechanism of CQDs/TiO<sub>2</sub> composite photocatalyst.

Zhang et al. prepared CQDs using base-assisted electrochemical method by carbon source of graphite rods [66]. The resulted CQDs was employed to make CQDs/Ag<sub>3</sub>PO<sub>4</sub> and CQDs/Ag<sub>3</sub>PO<sub>4</sub>/Ag composite photocatalyst for the photocatalysis of methyl orange. The results show the catalytic efficiency of CQDs/Ag<sub>3</sub>PO<sub>4</sub> and CQDs/Ag<sub>3</sub>PO<sub>4</sub>/Ag for methyl orange is significantly higher than that of Ag<sub>3</sub>PO<sub>4</sub> and Ag<sub>3</sub>PO<sub>4</sub>/Ag. The analysis of degradation mechanism indicates that the existence of CQDs can provide the following role: significantly reducing the water solubility of catalyst; acting as electron donors and acceptors and transferring electrons on the surface of the catalyst; enhancing catalyst stability and corrosion resistance; adding up-conversion performance and capturing electrons as an electron pool; reducing the recombination rate of photogenerated electron/hole pairs. The Fig. 9 shown the catalysis mechanism of CQDs/Ag<sub>3</sub>PO<sub>4</sub> composite photocatalyst.

Although CQDs has shown certain effects in the photocatalysis, the preparation process of CQDs composite catalysts is relatively more complicated. Therefore, simplifying the preparation method and realizing the in-situ synthesis of CQDs composite catalysts are of great significance and should be focused in future research.

## 4. Applications of CQDs fluorescence probe

### 4.1. The application of CQDs as the fluorescence probe

Fluorescence probe is a convenient, simple method with the advantage of easiness of operate good selectivity and high sensitivity. It is commonly used in the real-time detection and in-situ detection of various metal ions. Compared to traditional fluorescence probe, CQDs fluorescence probe is no toxic and greener. Therefore, the CQDs fluorescence probe has been developed widely for metal ion and medicinal detection[42, 67-70]. The Fig. 10 shows the detection of various quencher using CQDs fluorescence probe.

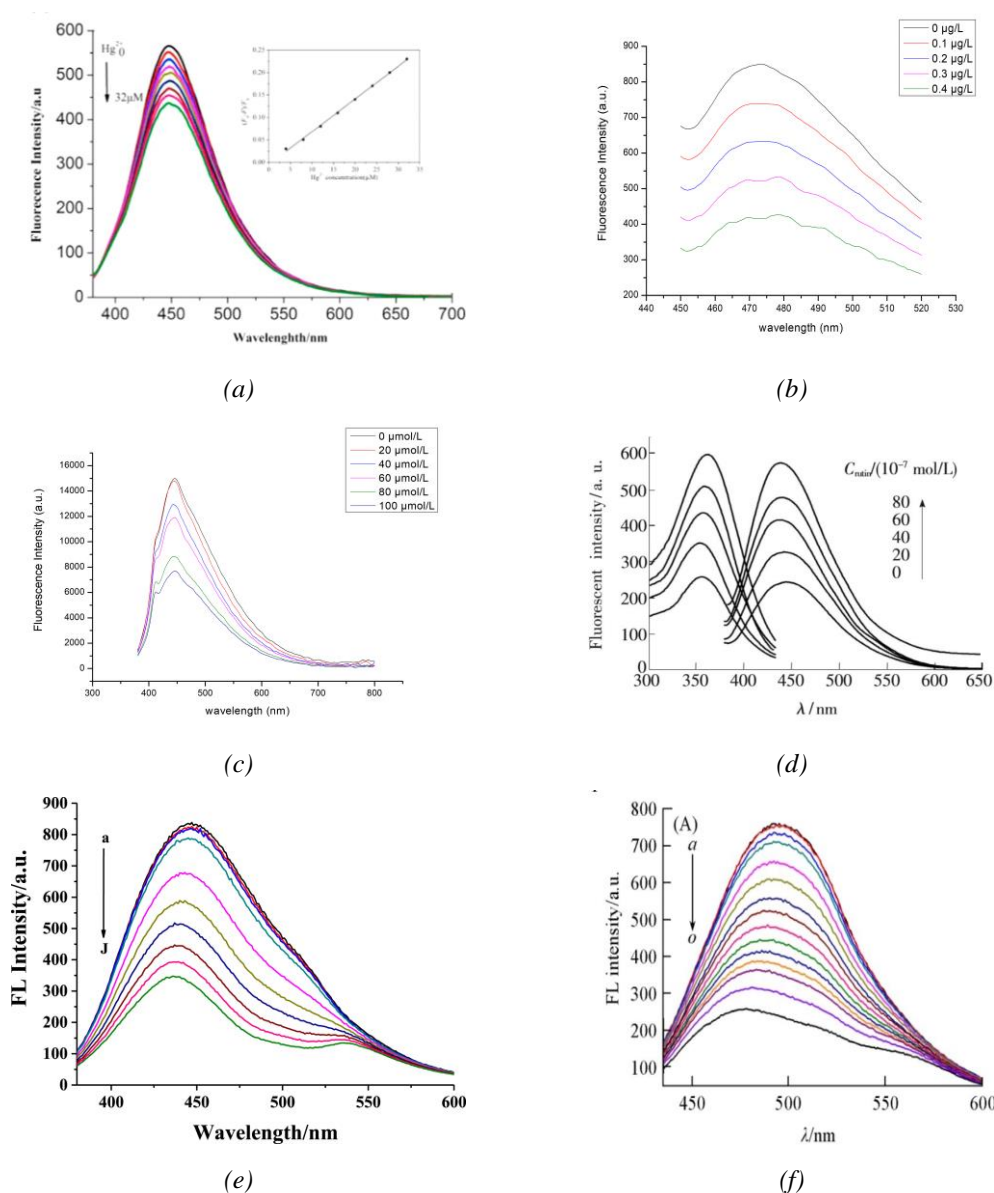


Fig. 10. The detection of various quencher using CQDs fluorescence probe: (a)  $Hg^{2+}$ , (b)  $Cr^{6+}$ , (c)  $Fe^{3+}$ , (d) rutin, (e) Sudan I and (f) Carmine.

## 4.2. The mechanism of fluorescence quenching

In this article, we mainly make a detailed introduction to the fluorescence quenching, which is rarely involved in the previous review. This helps us better understand the working principle of CQDs fluorescence probe. There are three main theories for fluorescence quenching of CQDs.

### 4.2.1. Fluorescence resonance energy transfer

Fluorescence energy resonance transfer (FERT) is a kind of energy transfer phenomenon between two fluorescent molecules that are close together. When the emission spectrum of the donor fluorescent molecule overlaps with the absorption spectrum of the acceptor fluorescent molecule, and the distance between the two molecules is within 10 nm, a non-radioactive energy transfer occurs, that is, the FRET phenomenon, which makes the fluorescence of the donor. The intensity is much lower than when it is alone (fluorescence quenching), but the fluorescence emitted by the acceptor is greatly enhanced (sensitized fluorescence)[71]. Usually, the quencher for detection and CQDs is acted as the acceptor and donor, respectively. The FERT effect can lead to the change of CQDs fluorescent lifetime after adding quencher[72].

### 4.2.2. Inner filter effect

The molecular spectrum is a band spectrum. If the Stokes shift is small, part of the fluorescence emission spectrum of CQDs will overlap with the fluorescence excitation spectrum of quencher, so part of the fluorescence emission will be reabsorbed. In this way, the fluorescence intensity will inevitably decrease, which is the inner filter effect[73]. Inner filter effect is a main reason for fluorescence quenching of CQDs.

### 4.2.3. Quenching effect rate

Quenching effect rate is explained by static quenching effect (SQE) or dynamic quenching effect (DQE) or simultaneously. DQE is a process in which the fluorescence intensity decreases due to the interaction between the quencher and the fluorescent excited state molecules of CQDs; SQE refers to the process in which the quencher and the ground state phosphor molecules of CQDs form a non-luminescent complex to reduce the decrease in fluorescence intensity

Both DQE and SQE through ground-state complex formation model can be described by the Stern–Volmer equation (equation 1)[74]:

$$F_0/F = 1 + K_{SV}c_q = 1 + K_q\tau_0c_q \quad (1)$$

where Here,  $F_0$  and  $F$  are the fluorescence intensity in the absence and presence of the quencher,  $K_{SV}$  is the quenching constant,  $\tau_0$  is the average lifetime of CQDs and  $K_q$  is the quenching rate constant. Compared to the maximum scatter collision quenching constant ( $1.0 \times 10^{10} \text{M}^{-1} \text{s}^{-1}$ ), the higher  $K_q$  value indicates the static quenching of CQDs. Quenching effect rate is used to illustrate the kinetics of quenching of CQDs.

## 5. Conclusions

Animal by-products are a very promising carbon source for the preparation of CQDs. However, this research is not comprehensive enough worldwide at present and can be studied in further.

High fluorescence of CQDs can hinder the Raman signal and cover the real value of signal. To develop a novel method to overcome this defect is desirable.

Up to date, amount of achievements have been obtained in CQDs fluorescence probe, the function of fluorescence probe is focus on detection of one quencher. The detection for two or more than two quenchers is meaningful and valuable.

## Acknowledgments

The authors sincerely thank the funds for Study on Comprehensive Control of Rocky Desertification and Ecological Service Function Improvement in Karst Peaks (No. 2016YFC0502402).

## References

- [1] X. Zhang, F. Wang, H. Huang, H. Li, X. Han, Y. Liu, Z. Kang, *Nanoscale* **5**(6), 2274 (2013).
- [2] D. Tang, J. Liu, X. Wu, R. Liu, X. Han, Y. Han, H. Huang, Y. Liu, Z. Kang, *Acs Appl. Mater. Interfaces* **6**(10), 7918 (2014).
- [3] Y. Zhu, X. Ji, C. Pan, Q. Sun, W. Song, L. Fang, Q. Chen, C. E. Banks, *Energy & Environmental Science* **6**(12), 3665 (2013).
- [4] Y. Dong, C. Chen, J. Lin, N. Zhou, Y. Chi, G. Chen, *Carbon* **56**(Complete), 12 (2013).
- [5] Z. Ma, Y. L. Zhang, L. Wang, H. Ming, H. Li, X. Zhang, F. Wang, Y. Liu, Z. Kang, S. T. Lee, *Applied Materials & Interfaces* **5**(11), 5080 (2013).
- [6] Y. Ma, X. Li, Z. Yang, S. Xu, Y. Zhang, *Langmuir* **32**(37), 9418 (2016).
- [7] P. J. Lai, S. G. Harroun, S. Y. Chen, B. Unnikrishnana, C. C. Huang, *Sensors & Actuators B Chemical* **228**, 465 (2016).
- [8] J. Tan, R. Zou, J. Zhang, W. Li, D. Yue, *Nanoscale* **8**(8), 4742 (2016).
- [9] X. Luo, P. x. Bai, X.-c. Wang, G. Zhao, H. Ren, *New Journal of Chemistry* **43**(14) (2019).
- [10] Y. Xu, X. H. Jia, X. B. Yin, X. W. He, Y. K. Zhang, *Analytical Chemistry* **86**(24), 12122 (2014).
- [11] S. Paulo, E. Palomares, E. Martinezferrero, *Nanomaterials* **6**(9), 157 (2016).
- [12] H. Zheng, N. Ping, Z. Zhao, *Rsc Advances* **7**(43), 26943 (2017).
- [13] S. Zhao, C. Li, L. Wang, N. Liu, Z. Kang, *Carbon*, **99**, 599 (2015).
- [14] H. Ren, G. Lin, G. Qian, L. Lu, J. Li, *RSC Advances* **8**(36), 20157 (2018).
- [15] J. Chen, X. Jiang, C. Zhang, K. R. Mackenzie, F. Stossi, T. Palzkill, M. C. Wang, W. Jin, *ACS Sensors* **2**(9), 1257 (2017).
- [16] G. Jiang, G. Zeng, W. Zhu, Y. Li, X. Dong, G. Zhang, X. Fan, J. Wang, Y. Wu, B. Z. Tang, *Chemical Communications* **53**(32), 4505 (2017).

- [17] *Sensors & Actuators B Chemical*, **217**, 198.
- [18] L. Fang, L. Zhang, Z. Chen, C. Zhu, J. Liu, J. Zheng, *Materials Letters* **191**, 1.
- [19] P. D., S. Saini, A. Thakur, B. Kumar, S. Tyagi, M. K. Nayak, *Journal of Hazardous Materials* **328**, 117.
- [20] R. Das, R. Bandyopadhyay, P. Pramanik, *Materials Today Chemistry* **8**, 96.
- [21] Y. Zhang, K. Liu, L. Meng, *Materials Review* (2017).
- [22] S. Zhu, Y. Song, X. Zhao, J. Shao, J. Zhang, Y. Bai, *Nano Research* **8**(2), 355 (2015).
- [23] K. Dimos, *Current Organic Chemistry* **20**(6), (2016).
- [24] L. Craco, S. S. Carara, T. A. D. S. Pereira, M. V. Milošević, *Phys. Rev. B* **93**(15), 155417 (2016).
- [25] X. Zhou, Z. Tian, J. Li, H. Ruan, Y. Ma, Z. Yang, Y. Qu, *Nanoscale* **6**(5), 2603 (2014).
- [26] H. Xu, S. Zhou, L. Xiao, H. Wang, S. Li, Q. Yuan, *Journal of Materials Chemistry C* **3**(2), 291 (2014).
- [27] Q. Zhang, X. Sun, H. Ruan, K. Yin, H. Li, *Science China Materials* **60**(2), 141 (2017).
- [28] Y. Li, B.-P. Zhang, J.-X. Zhao, Z.-H. Ge, X.-K. Zhao, L. Zou, *Applied Surface Science* **279**(9), 367 (2013).
- [29] Q. Wang, H. Wang, D. Liu, P. Du, P. Liu, *Synthetic Metals* **231**(5), 120 (2017).
- [30] P. Lv, Y. Yao, H. Zhou, J. Zhang, Z. Pang, K. Ao, Y. Cai, Q. Wei, *Nanotechnology* **28**(16), 165502 .
- [31] H. Bozetine, Q. Wang, A. Barras, M. Li, T. Hadjersi, S. Szunerits, R. Boukherroub, *Journal of Colloid & Interface Science* **465**, 286 (2016).
- [32] S. Mitra, S. Chandra, S. H. Pathan, N. Sikdar, P. Pramanik, A. Goswami, *RSC Advances* **3**(10), 3189 (2013).
- [33] A. Mewada, S. Pandey, S. Shinde, N. Mishra, G. Oza, M. Thakur, M. Sharon, M. Sharon, *Mater. Sci. Eng. C Mater. Biol. Appl.* **33**(5), 2914 (2013).
- [34] R. Atchudan, S. Perumal, R. Vinodh, R. L. Yong, *Journal of Alloys & Compounds*, S0925838818323934 (2018)
- [35] X. Yang, Y. Zhuo, S. Zhu, Y. Luo, Y. Feng, Y. Dou, *Biosensors & Bioelectronics* **60**(60), 292 (2014).
- [36] J. Wang, D. C.-F. Wang and P. S. Chen, *Angewandte Chemie International Edition* **51**(37), 9431.
- [37] P. Y. Lin, C.-W. Hsieh, M.-L. Kung, L.-Y. Chu, H.-J. Huang, H.-T. Chen, D.-C. Wu, C.-H. Kuo, S.-L. Hsieh, S. Hsieh, *Journal of Biotechnology* **189**, 114.
- [38] W. Li, Z. H Susan, *Analytical Chemistry* **86**(18), 8902 (2014).
- [39] Y. Hao, Z. Gan, J. Xu, X. Wu, P. K. Chu, *Applied Surface Science* **311**(9), 490 (2014).
- [40] V. S. Gorelik, Y. P. Voinov, G. A. Emel'chenko, V. M. Masalov, *Inorganic Materials* **46**(5), 505 (2010).
- [41] X. Lu, Z. Zhang, Q. Xia, M. Hou, C. Yan, Z. Chen, Y. Xu, R. Liu, *Materials Science & Engineering C* **82**, (2018).
- [42] C. Cheng, Y. Shi, M. Li, M. Xing, Q. Wu, *Materials Science and Engineering: C* **79**, 473 (2017).
- [43] Y. Liu, N. Peard, J. C. Grossman, *Journal of Physical Chemistry Letters* **10**(13), (2019).
- [44] S. Sun, X. Song, Y. Sun, D. Deng, Z. Yang, *Catalysis Science & Technology* **2**(5), 925 (2012).
- [45] J. Villaseñor, H. D. Mansilla, *Journal of Photochemistry & Photobiology A Chemistry* **93**(2),

- 205 (1996).
- [46] S. Mandani, B. Sharma, D. Dey, T. K. Sarma, RSC Advances, 10.1039.C1036RA17306C.
- [47] Y. Zhang, J. Zhang, J. Zhang, S. Lin, Y. Huang, R. Yuan, X. Liang, W. Xiang, Dyes & Pigments **140**, 122.
- [48] W. U. Khan, D. Wang, Y. Wang, Inorganic Chemistry.
- [49] V. Arul, M. G. Sethuraman **78**, 181 (2018).
- [50] L. Jing, J. Song, X. Liang, M. Qi, F. Feng, Analytical Methods **9**(45), (2017).
- [51] X. Deng, Y. Feng, H. Li, Z. Du, H. Wang, Particuology, (2018).
- [52] Y. Zhao, Y. Zhang, X. Liu, H. Kong, Y. Wang, G. Qin, P. Cao, X. Song, X. Yan, Q. Wang, Scientific Reports **7**(1), 4452 (2017).
- [53] Z. X. Liu, B. B. Chen, M. L. Liu, H. Y. Zou, C. Z. Huang, Green Chemistry **19**, (2017).
- [54] M. Wu, Y. Wang, W. Wu, C. Hu, X. Wang, J. Zheng, Z. Li, B. Jiang, J. Qiu, Carbon **78**, 480.
- [55] G. Zhang, L. Hu, K. Zhu, M. Yan, J. Liu, J. Yang, H. Bi, Applied Surface Science **364**, 660 (2016).
- [56] S. Zhu, Q. Meng, L. Wang, J. Zhang, Y. Song, H. Jin, K. Zhang, H. Sun, H. Wang, B. Yang, Angewandte Chemie International Edition **52**(14), 3953 (2013).
- [57] P. Dan, X. Li, A. Zhang, Applied Surface Science **427**, (2018).
- [58] V. Arul, T. N. Edison, Y. R. Lee, M. G. Sethuraman, Journal of Photochemistry & Photobiology B Biology **168**, 142 (2017).
- [59] V. Arul, M. G. Sethuraman, Optical Materials **78**, 181 (2018).
- [60] L. Kong, G. Duan, G. Zuo, W. Cai, Z. Cheng, Materials Chemistry & Physics **123**(2), 421 (2010).
- [61] Y. Han, H. Hui, H. Zhang, L. Yang, H. Xiao, R. Liu, H. Li, Z. Kang, Acs Catalysis **4**(3), 781 (2014).
- [62] S. Li, S. Zhou, H. Xu, L. Xiao, W. Yi, H. Shen, H. Wang, Q. Yuan, Journal of Materials Science **51**(14), 6801 (2016).
- [63] A. Bhati, S. R. Anand, G. Kumar, A. Garg, P. Khare, S. K. Sonkar, ACS Sustainable Chemistry & Engineering (2018).
- [64] T. C. Araújo, H. D. S. Oliveira, J. J. S. Teles, J. D. Fabris, L. C. A. Oliveira, J. P. D. Mesquita, Applied Catalysis B Environmental **182**, 204 (2016).
- [65] D. Hazarika, N. Karak, Applied Surface Science **376**, 276 (2016).
- [66] H. Zhang, H. Huang, H. Ming, H. Li, L. Zhang, Y. Liu, Z. Kang, Journal of Materials Chemistry **22**(21), 10501 (2012).
- [67] H. Huang, Y. Weng, L. Zheng, B. Yao, W. Weng, X. Lin, Journal of Colloid & Interface Science **506**, 373.
- [68] L. Lei, F. Wang, Y. Lv, J. Liu, Z. Shao.
- [69] Q. Qu, A. Zhu, X. Shao, G. Shi, Y. Tian, Chemical Communications **48**(44), 5473.
- [70] Z. Li, Y. Zhang, Q. Niu, M. Mou, Y. Wu, X. Liu, Z. Yan, S. Liao, Journal of Luminescence **187**, 274.
- [71] S. Gogoi, R. Khan, Physical Chemistry Chemical Physics **20**(24), (2018).
- [72] S. Hu, Q. Zhao, Q. Chang, J. Yang, J. Liu, RSC Advances **4**(77), 41069.
- [73] N. Shao, Y. Zhang, S. Cheung, R. Yang, W. Chan, T. Mo, K. Li, F. Liu, Analytical Chemistry **77**(22), 7294.
- [74] J. R. L, Principles of Fluorescence Spectroscopy, 1999.